Electron-Spin Distribution in Radical Anions of Aryl Methyl Ethers vs Reactivity and Regioselectivity of Their Unimolecular Fragmentation

M. Celina R. L. R. Lazana, M. Luisa T. M. B. Franco, and Bernardo J. Herold*

Contribution from the Instituto Superior Técnico, Laboratório de Química Orgânica, Av. Rovisco Pais, P-1096 Lisboa Codex, Portugal. *Received February 23, 1989*

Abstract: Seven different aryl methyl ethers (**1-7**) were reduced by Li, Na, K, and Cs in THF, DME, or mixtures of THF and DME. The resulting solutions were studied by ESR and, in some cases (**5-7**), by ENDOR and TRIPLE. With the exception of **3** and **4**, the resulting $ROAr^{\bullet-}M^+$ radicals could be observed. The experimental electron-spin distributions (including those published for other ethers) were compared with the results of the Hückel-McLachlan and INDO calculations. These combined results and the temperature variation for $6^{\bullet-}M^+$ allowed us to establish the conformations of $ROAr^{\bullet-}$ and the localization of M^+. The persistence of $ROAr^{\bullet-}$ toward OAr bond scission increases with the corresponding π-bond order and the oxygen metal distance. The orthogonal conformation favors RO-bond scission, the planar one OAr-bond scission. A new way to understand the influence of structure, conformation, counterion, and solvent on the reactivity and regioselectivity in unimolecular $ROAr^{\bullet-}M^+$ fragmentation is presented in terms of a single-step mechanism and by considering the lowering effect of the coulombic field of M^+ on the energies of the various species and states involved.

Recent publications on alkyl aryl ether cleavage by alkali metals[1,2] and by electrolytical reduction,[3,4] as well as unpublished material and earlier literature, were reviewed by Maercker,[5] who also presents some new mechanistic views on this reaction. The first step leads to radical anions $ROAr^{\bullet-}$, known since 1968 from ESR studies.[6] Dianions were also been discussed in the past as intermediates,[7-12] although the more recent literature[1,5,13-19] shows that in most cases this is an unnecessary hypothesis. Intermediates of the same type as $ROAr^{\bullet-}$ are important in $S_{RN}1$ reactions.[20,21] Therefore, it seemed appropriate to continue the existing ESR studies of radical anions $ROAr^{\bullet-}$[1,6,14,22-26] and of diaryl ethers[13,25,26] by a more careful examination. We now present an ESR, ENDOR, and TRIPLE resonance study of the reduction of ethers **1-7** with alkali metals in view of a more complete interpretation of the reactivity and regioselectivity in the fragmentation of such species.

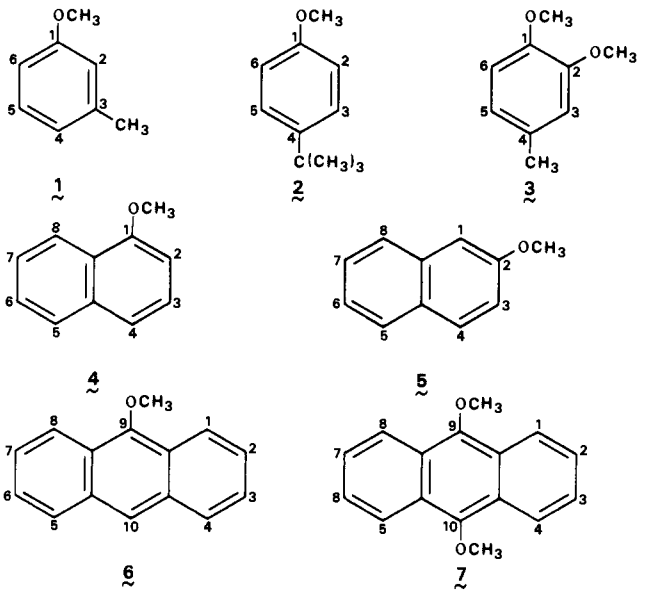

Experimental Results and Discussion

The substituted anisoles **1-3** were reduced with Na-K alloy in THF, DME, or mixtures of THF and DME at temperatures near the freezing point of the solvent. The ESR spectra were recorded at temperatures ranging from 163 K to room temperature.

By reduction of 3-methylanisole (**1**) and 4-*tert*-butylanisole (**2**), spectra of their structurally unchanged radical anions were observed at temperatures ranging from 163 to 183 K. The hyperfine splitting constants (hsc's) shown in Table I, were obtained by

(1) Lazana, M. C.; Franco, M. L.; Herold, B. J.; Maercker, A. IX Encontro Anual da Sociedade Portuguesa de Química, Estrutura e Reactividade Molecular, Coimbra, Portugal, 1986; Communication 8 CP 15.

(2) Maslak, P.; Guthrie, R. D. *J. Am. Chem. Soc.* **1986**, *108*, 2628, 2637.

(3) Thornton, T. A.; Woolsey, N. F.; Bartak, D. E. *J. Am. Chem. Soc.* **1986**, *108*, 6497.

(4) Pacut, R. l.; Kariv-Miller, E. *J. Org. Chem.* **1986**, *51*, 3468.

(5) Maercker, A. *Angew. Chem., Int. Ed. Engl.* **1987**, *26*, 972. For a more complete coverage of the period before 1965, see earlier reviews quoted in this one.

(6) Bowers, K. W. In *Radical Ions*; Kaiser, E. T., Kevan, L., Ed.; Wiley Interscience: New York, 1968; p 232.

(7) Birch, A. J. *J. Chem. Soc.* **1944**, 430.

(8) Birch, A. J. *J. Chem. Soc.* **1947**, 102.

(9) Eisch, J. J. *J. Org. Chem.* **1963**, *28*, 707.

(10) Normant, H.; Cuvigny, T. *Bull. Soc. Chim. Fr.* **1966**, 3344.

(11) Testaferri, L.; Tiecco, M.; Tingoli, M.; Chianelli, D.; Montanucci, M. *Tetrahedron* **1982**, *38*, 3687.

(12) Itoh, M.; Yoshida, S.; Ando, T.; Miyaura, N.; *Chem. Lett.* **1976**, 271.

(13) Evans, A. G.; Roberts, P. B.; Tabner, B. J. *J. Chem. Soc. B* **1966**, 269.

(14) Brown, J. K.; Burnham, D. R.; Rogers, N. A. J. *J. Chem. Soc. B* **1969**, 1149.

(15) Screttas, C. G. *J. Chem. Soc., Chem. Commun.* **1972**, 869.

(16) Rossi, R. A.; Bunnett, J. F. *J. Am. Chem. Soc.* **1972**, *94*, 683.

(17) Santiago, E.; Simonet, J. *Electrochim. Acta* **1975**, *20*, 853.

(18) Patel, K. M.; Baltisberger, J. R.; Stenberg, V. I.; Woolsey, N. F. *J. Org. Chem.* **1982**, *47*, 4250.

(19) Koppang, M. D.; Woolsey, N. F.; Bartak, D. E. *J. Am. Chem. Soc.* **1984**, *106*, 2799.

(20) Bunnett, J. F. *Acc. Chem. Res.* **1978**, *11*, 413.

(21) Rossi, R. A. *Acc. Chem. Res.* **1982**, *15*, 164.

(22) Tylli, H. *Suom. Kemisteseuran Tied.* **1973**, *82*, 70; *Chem. Abstr.* **1974**, *80*, 132506 f.

(23) Cerri, V.; Boyer, M.; Tordo, P. *Gazz. Chim. It.* **1985**, *115*, 147.

(24) Brown, J. K.; Burnham, D. R. *Mol. Phys.* **1968**, *15*(2), 173.

(25) Eargle, D. H., Jr. *J. Org. Chem.* **1963**, *28*, 1703.

(26) Literature on ESR of several radical anions $ROAr^{\bullet-}$ with strongly electron-withdrawing substituents can be found in: Landolt-Börnstein. *Magnetic Properties of Free Radicals*: Fischer, H., Hellwege, K.-H., Springer-Verlag: Berlin, Heidelberg, New York, 1977; Vol. 9, Part b; Vol. 9, Part d.

0002-7863/89/1511-8640$01.50/0

Table I. Experimental Hyperfine Splitting Constants and Theoretical Values According to Hückel–McLachlan Spin Density Calculations with Parameters Indicated for the Ion Pairs of 1, 2, and 5–7 (Q^H_{CH} = −2.3 mT; $Q^H_{COCH_3}$ = 0.23 mT)

	hsc, mT		
	exptl	calcd[a]	Hückel parameters
$1^{\bullet-}K^+$	a_2 = −0.343	a_2 = −0.386	δ_O = 3.0; γ_{CO} = 0.9; δ_2 = 0.05; δ_3 = −0.07;
	$a_3(CH_3)$ = 0.520	$a_3(CH_3)$ = 0.501	$\gamma_{1.2}$ = 1.03; $\gamma_{2.3}$ = 1.1; $\gamma_{3.4}$ = 0.98
	a_4 = −0.315	a_4 = −0.209	
	a_5 = −0.601	a_5 = −0.545	
	a_6 = −0.428	a_6 = −0.453	
$2^{\bullet-}K^+$[b]	$a_{2.6}$ = −0.522	$a_{2.6}$ = −0.658	δ_O = 3.0; γ_{CO} = 0.9; δ_2 or δ_6 = 0.05; δ_4 = −0.01
	$a_{3.5}$ = −0.602	$a_{3.5}$ = −0.686	
$5^{\bullet-}K^+$[c]	a_1 = −0.422	a_1 = −0.450	δ_O = 3.0; γ_{CO} = 0.9; δ_1 or δ_3 = 0.05; δ_2 = −0.017[d]
	$a_{H(o\text{-}CH_3)}$ = 0.009	$a_{H(o\text{-}CH_3)}$ = 0.007	
	a_3 = −0.342	a_3 = −0.194	
	a_4 = −0.498	a_4 = −0.533	
	a_5 = −0.545	a_5 = −0.546	
	a_6 = −0.055	a_6 = −0.054	
	a_7 = −0.321	a_7 = −0.166	
	a_8 = −0.422	a_8 = −0.481	
$6^{\bullet-}Na^+$[e,f]	$a_{1.8}$ = −0.290	$a_{1.8}$ = −0.322	δ_O = 3.1; γ_{CO} = 0.9; δ_1 = +0.2; δ_9 = δ_{10} = −0.2[d]
	$a_{2.7}$ = −0.152	$a_{2.7}$ = −0.086	
	$a_{3.6}$ = −0.152	$a_{3.6}$ = −0.090	
	$a_{4.5}$ = −0.290	$a_{4.5}$ = −0.319	
	a_{10} = −0.477	a_{10} = −0.457	
	$a_{H(o\text{-}CH_3)}$ = 0.015	$a_{H(o\text{-}CH_3)}$ = 0.049	
$6^{\bullet-}K^+$[e,g]	$a_{1.8}$ = −0.295	$a_{1.8}$ = −0.322	δ_O = 2.9; γ_{CO} = 0.9; δ_9 = δ_{10} = −0.1[d]
	$a_{2.7}$ = −0.141	$a_{2.7}$ = −0.050	
	$a_{3.6}$ = −0.173	$a_{3.6}$ = −0.113	
	$a_{4.5}$ = −0.277	$a_{4.5}$ = −0.275	
	a_{10} = −0.505	a_{10} = −0.473	
	$a_{H(o\text{-}CH_3)}$ = 0.017	$a_{H(o\text{-}CH_3)}$ = 0.057	
$6^{\bullet-}Cs^+$[e,g]	$a_{1.8}$ = −0.288	$a_{1.8}$ = −0.320	δ_O = 2.7; γ_{CO} = 0.9; δ_9 = δ_{10} = −0.08[d]
	$a_{2.7}$ = −0.146	$a_{2.7}$ = −0.048	
	$a_{3.6}$ = −0.165	$a_{3.6}$ = −0.115	
	$a_{4.5}$ = −0.288	$a_{4.5}$ = −0.271	
	a_{10} = −0.491	a_{10} = −0.472	
	$a_{H(o\text{-}CH_3)}$ = 0.015	$a_{H(o\text{-}CH_3)}$ = 0.055	
$7^{\bullet-}M^+$[e] (M = Li, Na, K, Cs)	$a_{1.4,5.8}$ = −0.304	$a_{1.4,5.8}$ = −0.313	δ_O = 2.5; γ_{CO} = 0.9; δ_9 = δ_{10} = −0.05[d]
	$a_{2.3,6.7}$ = −0.156	$a_{2.3,6.7}$ = −0.08	
	$a_{H(o\text{-}CH_3)}$ = −0.014	$a_{H(o\text{-}CH_3)}$ = 0.048	

[a] We have omitted in the table the INDO values since they do not differ substantially from the ones presented. [b] Reduction with Na–K alloy in a mixture of THF–DME (1:1). [c] Reduction with Na–K alloy in THF. [d] The resonance parameters γ_{CC} were corrected according to Streitwieser[32] for the standard geometry of the aromatic parent hydrocarbon. [e] Reduction in THF at 183 K. [f] Structure 1 of Figure 3 has been assumed. [g] Structure 2 of Figure 3 has been assumed.

successful simulation of the corresponding ESR spectra. The assignments were based on theoretical calculations as discussed later. Above 183 K, the intensities of the $1^{\bullet-}$ and $2^{\bullet-}$ signals decrease. While above 203 K the spectrum of $2^{\bullet-}$ disappears and no further paramagnetic species is detected, $1^{\bullet-}$ is gradually replaced by the ESR spectrum of the radical anion of toluene, which is persistent at temperatures below 253 K. According to an experiment reported earlier in the literature,[6] the decay of $1^{\bullet-}$ was too fast, however, to allow for observation of its ESR spectrum. This different result can be explained by slightly different experimental conditions.

In the reduction of 2-methoxy-4-methylanisole (**3**), the primary radical anion, $3^{\bullet-}$, is not observed. Instead, the radical anion of 4-methylanisole resulting from Ar–O cleavage in position 2 is observed. The ESR signal disappears above 203 K. One can therefore conclude that $1^{\bullet-}$ and $3^{\bullet-}$ undergo Ar–O bond scission, and $2^{\bullet-}$ probably does too because the radical anion of *tert*-butylbenzene may be difficult to obtain.

Although the reduction of 1-methoxynaphthalene (**4**) with either Na, K, or Cs in THF gives immediately the naphthalene radical anion, 2-methoxynaphthalene (**5**) gives by reduction under the same conditions its radical anion, $5^{\bullet-}$. The ESR spectra obtained have a very complex hyperfine structure owing to the low symmetry of this species. This radical anion fortunately could also be studied by ENDOR and general TRIPLE resonance, which allowed for the determination of seven different proton hsc's and their relative signs, according to well-known criteria.[27] In the ion pair $5^{\bullet-}Cs^+$, a cesium hsc is observed (a_{Cs} = 0.123 mT), which is confirmed by spectral simulation. Above 203 K, the naphthalene radical anion with its counterion $Nph^{\bullet-}$ M^+ (Nph = naphthalene) begins to appear superimposed with $5^{\bullet-}M^+$, and at room temperature $Nph^{\bullet-}M^+$ becomes the dominating species, with any of the alkali metals studied.

Unlike compounds **1**–**5**, which are not reduced by lithium at low temperatures, 9-methoxyanthracene (**6**) and 9,10-dimethoxyanthracene (**7**) immediately give paramagnetic solutions by reaction with any of the alkali metals. When **6** is reduced with Li powder in THF or DME at about 173 K, the ESR of $Ant^{\bullet-}Li^+$ (Ant = anthracene) is immediately observed. The reduction with the remaining alkali metals leads to the respective radical anion $ROAr^{\bullet-}$, with increasing lifetimes from sodium to potassium and cesium. Thus, the ESR spectra of $6^{\bullet-}Cs^+$ are even observed at room temperature. At room temperature, asymmetric line broadening is evident in the ESR spectra of these ion pairs, denoting a dynamic effect, which suggests an intramolecular cation exchange between two positions. At this temperature, these ion pairs decompose slowly. Their ESR spectra are gradually replaced by the $Ant^{\bullet-}M^+$ spectra. The ESR studies of the radical anions $6^{\bullet-}$ have been completed by ENDOR and general TRIPLE resonance, allowing relative signs to be assigned to each coupling constant. The spin distribution is dependent on the cation (see Table I), but the variation is not linearly related to the cationic radius as in the case of other series of ion pairs.[28] Particularly

(27) Kurreck, H.; Kirste, B.; Lubitz, W. *Angew. Chem., Int. Ed. Engl.* **1984**, *23*, 173.

(28) Lazana, M. C. R. L. R.; Franco, M. L. T. M. B.; Herold, B. J. *J. Chem. Soc., Perkin Trans. 2* **1987**, 1399. Franco, M. L. T. M. B.; Lazana, M. C. R. L. R.; Herold, B. J. *J. Chem. Soc., Perkin Trans. 2* **1987**, 1407.

Table II. Decay of Alkali Metal Methyl Aryl Radical Anion Pairs ($ROAr^{\bullet-}M^+$) from the Observation of ESR Signals vs the π-Bond Order (p_{CO}) of ArO and the Energy of the Semioccupied Molecular Orbital SOMO (Coefficient m in $E = \alpha + m\beta$)[a]

	$ROAr^{\bullet-}$ decay bond	$HAr^{\bullet-}$ spectrum obsd	ArO bond scission assumed	p_{CO}	SOMO
anisole radical anion-K^+	yes, slow[6]	no(?), but instead Ar-$Ar^{\bullet-}$[6]	yes, fast	0.19	−1.03
1$^{\bullet-}K^+$	yes, slow	yes	yes, slow	0.19*	−1.05*
4-methylanisole radical anion-K^+	yes, slow	no	yes(?), slow	0.21*	−0.99*
2$^{\bullet-}K^+$	yes, slow	no	yes(?), slow	0.22*	−0.99*
1,2-dimethoxybenzene radical anion-K^+	too fast[6]	yes[6]	yes, fast	0.19	−1.03
1,3-dimethoxybenzene radical anion-K^+	too fast[6]	yes[6]	yes, fast	0.16	−1.06
1,4-dimethoxybenzene radical anion-K^+	yes, slow[6]	no[6]	yes(?), slow	0.21*	−1.00*
3$^{\bullet-}K^+$ C_2O	too fast	yes	yes, fast	p_{C_2O} 0.17	−1.03
C_1O	no	no	no(?)	p_{C_1O} 0.20	
4-nitroanisole radical anion-K^+	no[26]	no[26]	no	0.46*	−0.42*
4-methoxybiphenyl radical anion-K^+	too fast[6]	yes[6]	yes, fast	0.18	−0.74
2,2′-dimethoxybiphenyl radical anion-K^+	too fast[22]	yes[22]	yes, fast	0.18	−1.04
4,4′-dimethoxybiphenyl radical anion-K^+	yes, slow[22]	yes[22]	yes, slow	0.19*	−0.78*
4$^{\bullet-}Na^+$, K^+, or Cs^+	too fast	yes	yes, fast	0.18	−0.70
5$^{\bullet-}Na^+$, K^+ or Cs^+	yes, slow	yes	yes, slow	0.20*	−0.68*
6$^{\bullet-}Li^+$	too fast	yes	yes, fast	0.18	−0.56
6$^{\bullet-}Na^+$	yes, slow	yes	yes, slow	0.19*	−0.56*
6$^{\bullet-}K^+$	yes, slow	yes	yes, slow	0.19*	−0.55*
6$^{\bullet-}Cs^+$	yes, slow	yes	yes, slow	0.20*	−0.55*
7$^{\bullet-}Li^+$	yes, slow	yes	yes, slow	0.19*	−0.61*
7$^{\bullet-}Na^+$, K^+, or Cs^+	yes, slow	no	no	0.19*	−0.61*
BMPMF$^{\bullet-}K^+$[b,34]	no	no	no	0.21*	−0.36*

[a] Values marked with an asterisk were calculated with the help of parameters adjusted to match those calculated with experimental spin densities. The others were calculated using parameters for the most similar radical anion marked with an asterisk. For 2,2′-dimethoxybiphenyl radical anion-K^+, due to the repulsion of the substituents $\gamma_{C_1C_1} = 0.2$ was taken for the central bond. [b] 9-Bis(4-methoxyphenyl)methylenefluorene.

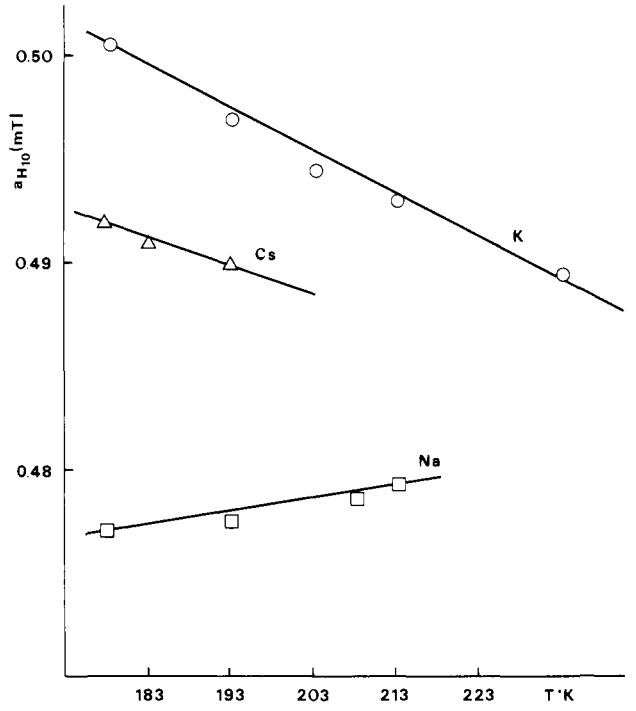

Figure 1. Experimental values of hyperfine splitting constant $a_{H_{10}}$ for ion pairs **6**$^{\bullet-}M^+$ (M = Na, K, Cs) as a function of temperature.

for $a_{H_{10}}$, it goes through a maximum for the potassium ion pairs ($a_{H_{10}}$ = 0.477 mT for **6**$^{\bullet-}Na^+$, 0.505 mT for **6**$^{\bullet-}K^+$, and 0.491 mT for **6**$^{\bullet-}Cs^+$).

The temperature dependence observed for $a_{H_{10}}$ hsc's in the different ion pairs is depicted in Figure 1. The opposite behavior of the sodium ion pair as compared to the potassium and cesium ones and the nonmonotonic dependence of $a_{H_{10}}$ hsc's from the ionic radius of the cation must be due to a different structure of the ion pairs, as will be discussed later. The spectra of the **7**$^{\bullet-}M^+$ ion pairs (M = Li, Na, K, Cs) in THF or DME were all recorded in the temperature range from 173 K to room temperature. The proton hsc's were obtained by ENDOR and general TRIPLE resonance (see Table I). They are independent of either the counterion, the solvent, or the temperature. In **7**$^{\bullet-}Cs^+$, a cesium hsc can be observed (a_{Cs} = 0.44 mT).

Table III. Experimental and Calculated Hyperfine Splitting Constants for Anisole Radical Anion

	hsc, mT		
	2.6	3.5	4
exptl[a]	0.536	0.618	0.061
McLachlan[a,b]	−0.679	−0.676	0.204
McLachlan[b,c]	−0.658	−0.685	0.201
INDO[d]	−0.591	−0.647	0.194

[a] Reference 24. [b] Q^H_{CH} = −2.3 mT. [c] δ_O = 3.0; γ_{CO} = 0.9; δ_2 = 0.05. [d] Standard geometry for the benzene ring was assumed. The hsc were taken as the average of the hsc's computed for the orthogonal and planar conformations of the methoxyl group.

While for the ion pair **7**$^{\bullet-}Li^+$ some O–Ar cleavage leading to anthracene has been observed indirectly (through the ESR of Ant$^{\bullet-}Li^+$), in the ion pairs **7**$^{\bullet-}Na^+$ and **7**$^{\bullet-}Cs^+$ a diamagnetic solution is obtained, which can be taken as evidence for exclusive R–O-bond scission, yielding phenolates. The presence of phenols after hydrolysis was confirmed by the colorimetric test with the 4-aminoantipyrine reagent.[29] Potassium ion pairs **7**$^{\bullet-}K^+$ besides phenolates, detected after hydrolysis, by the same test for phenols, yield also an unknown paramagnetic species. ENDOR and TRIPLE resonance spectra of this radical allowed for the determination of five different negative proton hsc's, which is however not sufficient to assign the correct structure unambiguously.

Table II summarizes the observations on the relative persistence of the radical anions **1**$^{\bullet-}$ to **7**$^{\bullet-}$ together with other results.

Theoretical Calculations

Spin densities calculated by the Hückel-McLachlan method have been used in the theoretical interpretation of the hyperfine structure observed in the ESR spectra of radical ions of a large number of aromatic systems. The assignment of hsc's is frequently supported only by these calculations. However, spin densities calculated by Brown and Burnham for the anisole radical anion using this method estimate a larger hsc for the ortho position than for the meta position (Table III). These results are in opposition to what has been observed experimentally through the reduction

(29) Weiss, F. T. *Determination of Organic Compounds: Methods and Procedures*; Wiley-Interscience: New York, London, Sydney, Toronto, 1970; Vol. 32, p 177.

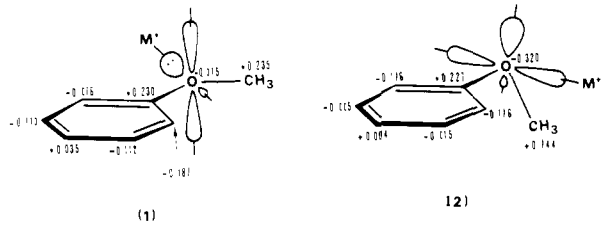

Figure 2. Excess charge distribution for the planar (1) and orthogonal (2) conformations of the radical anion of anisole, obtained from INDO calculations.

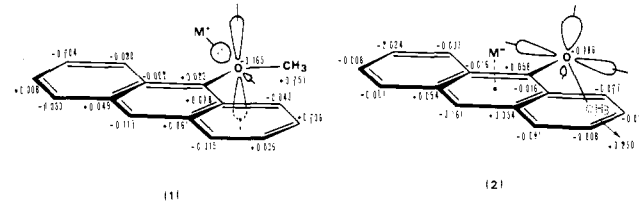

Figure 3. Excess charge distribution for the planar (1) and orthogonal (2) conformations of the radical anion of 9-methoxyanthracene ion pair $\mathbf{6}^{\bullet-}M^+$, from INDO calculations.

of selectively deuterated anisoles.[24] The possibility of rotational isomerism in alkyl aryl ether radical anions is responsible for the difficulty to correlate the experimental data with the theoretical results. In each conformer, the counterion must be placed near the center with the highest negative charge density.

A more convenient method to calculate spin densities in these systems, without excessive computational effort, would be the INDO (intermediate neglect of differential overlap) method. In spite of being a semiempirical method, all the valence shell electrons are included. Also, in order to take some account of exchange terms, all the differential overlap one-center integrals are equally considered. INDO is an approximate self-consistent field method that takes explicitly account of electrostatic effects of ionic and polar groups. The calculations were performed for the orthogonal and planar conformations of the methoxyl group with respect to the aromatic ring and the final spin distribution was taken as the average of the spin densities computed for each rotamer. Furthermore the calculated binding energy allows for the determination of the stability of the different conformational isomers. Such calculations were made for all new radical anions ($\mathbf{1}^{\bullet-}$, $\mathbf{2}^{\bullet-}$, $\mathbf{5}^{\bullet-}$, $\mathbf{6}^{\bullet-}$, and $\mathbf{7}^{\bullet-}$) whose ESR spectra were measured. However, for the sake of brevity, only those INDO results will be mentioned that differ from or add something new to the Hückel–McLachlan spin density calculations for the same radical anions. INDO calculations for the radical anion of anisole, assuming a standard geometry for the benzene ring, give, e.g., better agreement with experiment than the previous Hückel–McLachlan calculations. The calculated hsc's have magnitudes in the correct order (meta > ortho > para) (Table III). These hsc's are calculated by the average of the values obtained for the planar (1) conformation of the methoxyl group and for the orthogonal (2) one as represented in Figure 2.

According to these calculations, the energy of the orthogonal conformation (2) is only about 0.3 kJ mol^{-1} higher than for the planar conformation (1). According to MINDO/3 calculations by O. Hofer,[30] however, the orthogonal conformation in the unreduced anisole molecule is about 5.4 kJ mol^{-1} higher in energy than the planar one (still about one-half of the rotation barrier obtained from experimental data by some other authors quoted by O. Hofer). This is consistent with the circumstance that the planar conformation (1) is less stabilized electronically in the radical anion than in the unreduced anisole because of the lower bond order of the aromatic C–O bond in the former, as can be easily concluded from a simple HMO calculation. The calculated (INDO) excess charge distribution is shown for each conformation. The highest excess negative charge is localized on the oxygen atom ($\simeq$30% of the total). The most probable site for the equilibrium position of the cation is therefore in both conformations adjacent to the methoxyl oxygen in the plane of the benzene ring, since out of the ring plane the oxygen conjugated with the aromatic π system has, according to Hückel calculations, a partial positive charge.

In order to take into account the structural requirements for anisole radical ion pairs in Hückel–McLachlan calculations, the Coulomb parameter of the atoms near the counterion must be adjusted. The calculations thus performed are indicated in Table III. They are consistent with the observed sequence in the Hückel–McLachlan hsc calculations for $\mathbf{1}^{\bullet-}$, based on regular geometry for the benzene ring, and do not reproduce the experimentally observed spin distribution. The simultaneous presence of two electron-donating substituent groups in **1** might be responsible for this discrepancy since a ring distortion may occur. The calculated values indicated in Table I represent a better agreement with the experimental results. They were obtained considering, besides an adjustment due to the site of the cation, also adjustments of the resonance integrals for the 1–2, 2–3, and 3–4 bonds. Each value obtained is the average of the calculated values for both positions of the cation in the nodal plane (correction of Coulomb integral for either C_2 or C_6). The best result is achieved by considering a 50% contribution of each conformer.

A much smaller perturbation on the structure of the benzene ring is expected by the substitution of a *tert*-butyl group in a low spin density position such as the para position of anisole. Theoretical (HMO and INDO) calculations for the spin distribution in $\mathbf{2}^{\bullet-}$, based on the standard geometry for the benzene ring, are consistent with the experimental results.

Hückel–McLachlan spin density calculations for $\mathbf{5}^{\bullet-}$ were based on the standard geometry for naphthalene.[31] Resonance integral parameters for the different bonds were adjusted by the correlation between these parameters and bond lengths according to A. Streitwieser.[32] The values indicated in Table I result from an average of the calculated values considering the two possible positions of the counterion in the nodal plane (adjustment of either δ_1 or δ_3).

INDO calculations performed for the free-radical anion of $\mathbf{6}^{\bullet-}$, based on the standard geometry of anthracene,[31] estimate a lower binding energy for the planar conformation (1) than for the orthogonal one (2) (Figure 3), showing that, contrary to all former methoxyarene radical anions mentioned, the orthogonal conformation of $\mathbf{6}^{\bullet-}$ is more stable than the planar one. The calculated difference in binding energy for the two conformations is about 192.4 kJ mol^{-1}. Steric interactions between the methyl group and the protons connected to C_1 or C_8 in the planar conformation (1) are most certainly responsible for this result. In the planar conformation, the cation will be situated in the nodal plane near to the oxygen atom (structure 1), whereas in the orthogonal conformation the counterion is situated above the middle ring, probably displaced from the center toward the carbon atom with the highest excess negative charge C_{10} (structure 2).

Hückel–McLachlan spin density calculations for $\mathbf{6}^{\bullet-}$ were based on the standard geometry for anthracene and are given in Table I. Resonance integrals were corrected as described for $\mathbf{5}^{\bullet-}$ and Coulomb integrals for positions near the cation were adjusted. The calculated a_{10} hsc's assuming the orthogonal conformation (2) for the ion pairs with the cation at different distances from C_{10} (variable δ_C) are plotted in Figure 4. Identically, Figure 5 represents the a_{10} hsc's calculated assuming the planar structure 1 for the ion pair with the cation at different distances from the oxygen atom (variable δ_O). These plots simulate the predictable temperature dependence for each ion pair structure because the

(30) Hofer, O. *Monatshefte Chem.*, **1978**, *109*, 405.

(31) Allen, F. H.; Kennard, O.; Watson, D. G.; Brammer, L.; Orpen, A. G.; Taylor, R. *J. Chem. Soc., Perkin Trans. 2* **1987**, S1.

(32) Streitwieser, A., Jr *Molecular Orbital Theory for Organic Chemists*; John Wiley & Sons, Inc.: New York, London, 1961; p 105.

(33) McClelland, B. J. *Trans. Faraday Soc.* **1961**, *57*, 1458.

(34) Franco, M. L. T. M. B.; Herold, B. J.; Evans, J. C.; Rowlands, C. C. *J. Chem. Soc., Perkin Trans. 2* **1988**, 443.

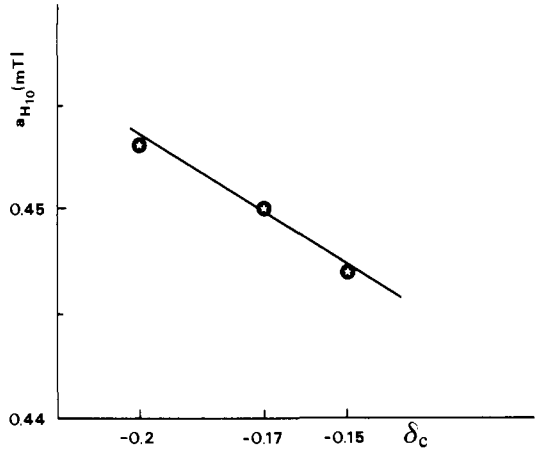

Figure 4. Calculated values for hyperfine splitting constant $a_{H_{10}}$ vs the Coulomb parameter of C_{10}, δ_C (used to simulate increasing temperature with increasing δ_C for the orthogonal conformation (2) of $6^{\bullet-}M^+$).

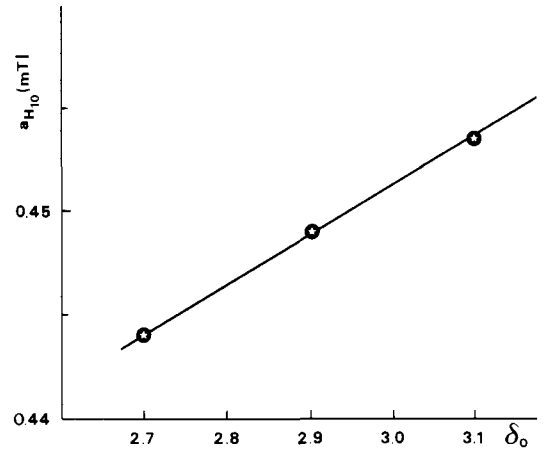

Figure 5. Calculated values for hyperfine splitting constant $a_{H_{10}}$ vs the Coulomb parameter of the oxygen atom, δ_O (used to simulate increasing temperature with increasing δ_O for the planar conformation (1) of $6^{\bullet-}M^+$).

interionic distance in arene radical anion pairs is known to decrease with increasing temperature and the Coulomb parameters according to McClelland[33] are inversely proportional to this distance.

The experimental results on the temperature dependence of $a_{H_{10}}$ described above are therefore reasonably explained if one assumes the orthogonal conformation (2) for the potassium and cesium ion pairs and the planar structure (1) for the observed sodium ion pairs. The high electrostatic interaction with the smaller cations may contribute to the decrease in the energy of the planar conformation relatively to the orthogonal one. Due to sterical hindrance by the hydrogen atoms connected to C_1 and C_8, the heavy alkali cations (K^+, Cs^+) cannot be localized near the negative charge concentration on oxygen in the plane of the ring system. The most probable equilibrium position of these cations is over the central ring, close to C_{10} as referred to above. The asymmetric line broadening observed for these ion pairs at room temperature may be related to the cation exchange between the position over the ring and the position in the nodal plane. The cation migration to the nodal plane seems, therefore, necessary to take place before the O–Ar bond scission can occur.

For the ion pairs $7^{\bullet-}$ M^+, where the hsc's are not dependent on the temperature and on the cation, the radical anion probably always has an orthogonal conformation with the counterion above the central ring.

INDO calculations, based on the standard geometry of anthracene, were performed for the two conformations of the ion pairs $7^{\bullet-}M^+$ with both of the OCH_3 groups either in the plane of the ring system or in the orthogonal plane. The comparatively high binding energy difference between the two conformations

Table IV. s-Orbital Spin Densities Calculated by INDO for the Orthogonal and Planar Conformations of Ion Pairs $7^{\bullet-}M^+$ [a]

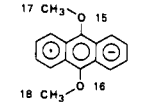

	s-orbital spin density		
	$10^2\rho_{sORTH}$	$10^2\rho_{sPL}$	ρ_{sORTH}/ρ_{sPL}
$C_{9,10}$	1.53	1.43	1.07
$O_{15,16}$	0.58	0.07	8.29
$C_{17,18}$	0.74	0.03	24.67

[a] The values for the other atoms have been omitted since they are irrelevant for the present discussion.

is consistent with the above observation. In effect, the orthogonal conformation is more stable than the planar one by 562.8 kJ mol^{-1}.

The hsc's, calculated by Hückel–McLachlan, for the orthogonal conformation, are given in Table I together with the experimental results. INDO calculated values are omitted in the table for the sake of brevity, but two points of interest must be mentioned: the negative sign of the hsc of the methyl hydrogens can be predicted by the INDO method, contrary to the Hückel–McLachlan calculations, and the possibility of calculating the spin distribution in the methoxyl groups for each conformation allows for the interpretation of the observed regioselectivity of the ArOR cleavage.

In effect, the most significant difference between the two conformations is the marked increase in the spin population in the methoxyl group in the orthogonal conformation. This is shown in Table IV where the s orbital spin density, ρ_s, calculated for the two conformations of the ion pairs $7^{\bullet-}M^+$, is given. The more than 20 times higher spin density in the R–O bond in the orthogonal conformation relates well to the observed increase in the amount of O–R bond scission in the ion pairs $7^{\bullet-}$ M^+, supporting the hypothesis above that O–Ar bond cleavage requires the association of the counterion with the oxygen atom in the nodal plane, whereas the O–R bond cleavage requires an orthogonal conformation of the methoxyl group.

The different stabilities observed for the radical anions obtained by reduction of alkyl aryl ethers with alkali metals seem to be related to the Ar–O bond order. The π-bond orders, p_{CO}, calculated by the Hückel method, measure the strength of the π bond due to the interaction of oxygen with the aromatic system (zero for a pure single bond and one for a full double bond). The values calculated for radical anions $1^{\bullet-}$–$7^{\bullet-}$ are shown in Table II. We have included in this table also the values calculated for the radical anions of some other alkyl aryl ethers with ESR spectra known from the literature, which are also of interest for the present discussion.

From the analysis of Table II, one can see that the higher the values calculated for the π-bond orders, p_{CO}, the longer is the lifetime of the radical anion $CH_3OAr^{\bullet-}$ observed experimentally.

For Ar–O π-bond p_{CO} orders lower than 0.19, no primary radical anion in any of the examples of the table has ever been observed, even at temperatures as low as 170 K. In order to observe such radicals, it is necessary that $p_{CO} \geq 0.19$. (Although a third calculated digit for p_{CO} is certainly meaningless in terms of absolute values, it was curious to verify that the highest value for the radicals that decompose too fast observed by ESR was 0.187 (2-methylanisole radical anion–K^+) and the lowest value for those that were observable was 0.189 ($6^{\bullet-}Na^+$), without any deliberate effort to adjust the parameters with the aim of provoking this separation.) Particularly interesting in this respect is the possibility of anticipating which of the ArO bonds is preferentially cleaved in the reduction of compounds like $3^{\bullet-}$. The calculated p_{CO} bond orders for $3^{\bullet-}$ are respectively 0.20 and 0.17 for the methoxyl group in positions 1 and 2. Since only for position 2 $p_{CO} < 0.19$, it can be predicted that the reduction of $3^{\bullet-}$ should lead to ArO bond scission in position 2 and, consequently, to 4-methylanisole. This is confirmed experimentally, as mentioned above, by the observation of the ESR spectrum of the radical anion of 4-methylanisole. The substitution of anisole in the para position by strong electron-withdrawing substituents such as NO_2 gives long-lived radical anions.[2,26] As in the former case, this is pre-

dictable theoretically because of the much higher p_{CO} bond order calculated for this compound (0.46) than for the remaining substituted anisoles. The calculated $p_{CO}\pi$-bond orders for the radical anions of 1- and 2-methoxynaphthalene, $\mathbf{4}^{\bullet-}$ and $\mathbf{5}^{\bullet-}$ explain the fast cleavage of the aryl oxygen bond in the reduction of **4** ($p_{CO} = 0.18 < 0.19$), thus precluding the observation of the primary radical anion, as compared to a much slower ArO bond cleavage in the radical anion of 5 where $p_{CO} = 0.20 > 0.19$ was calculated.

For the ion pairs $\mathbf{6}^{\bullet-}M^+$ (M = Li, Na, K, Cs), the calculated bond order increases (Table II) and the calculated SOMO energy decreases with the increasing size of the cation. These results correlate with the experimentally observed increase of the lifetime of the radical anions, $ROAr^{\bullet-}$ in the same order of the increasing cation radius.

Conclusions

Since well-resolved ESR spectra can only be obtained at high dilution, the observations on the decay of signals correspond to unimolecular reactions. Therefore, the present study confirms that radical anions obtained from alkali metal reduction of aryl methyl ethers undergo unimolecular fragmentation, which can take place both by ArO bond or CH_3O bond scission.

The rate of ArO bond scission increases with decreasing π-bond order of the ArO bond in the radical anion, which is a way to characterize the strength of this bond. There is a threshold value p_{CO} around 0.19 in the results of the calculations: below this value, the decay is so fast that the radical anion cannot be observed by conventional ESR measurements, and above, the radical anions of the aryl methyl ethers are sufficiently persistent to be observed by ESR.

The decay resulted almost always in ArO bond scission, possibly with an unknown extent of parallel CH_3O bond scission.

In all cases where ArO bond scission occurs, INDO calculations showed that the most stable conformation of the radical anion is the one where the CH_3O bond lies in the plane of the aromatic ring. The alkali-metal cation is then situated in the same plane adjacent to the oxygen atom in the direction of the nonbonding orbital as shown in Figures 2(1) and 3(1).

From the influence of the nature of the counterion on regioselectivity based on product analyses, as reported in the review by A. Maercker,[6] a rather confusing picture emerges. The decrease of the ArO bond scission rate in $\mathbf{6}^{\bullet-}M^+$ (**6** = 9-methoxyanthracene) with increasing ionic radius from M = Li to Cs is, however, a case where the INDO calculations show a charge concentration on oxygen, which is of the same order of magnitude as in ketyls where one has found[35] that the smaller the ionic radius, the shorter the oxygen metal distance. The influence of solvent reported by Maercker[5] for the cleavage of anisole and other ethers shows for less polar solvents (shorter oxygen–metal distances) an increase in the relative rate of OAr bond scission and in more polar solvents an increase of the relative rate of RO bond scission (more solvent-shared ion pairs, larger average oxygen–metal distances). Both the influence of the nature of the counterion and solvent point into the same direction: the shorter the oxygen–metal distance, the larger the relation between OAr and RO bond scission rates.

The temperature effects reported by Maercker[5] (increase of OAr vs RO bond scission rates with an increase of temperature) prove also that a shorter oxygen–metal distance causes an increase of OAr vs RO bond scission. Both the increase of the OAr vs RO bond scission rate and the absolute increase of the OAr bond scission rate with a stronger coulombic interaction with the radical anion can be easily rationalized if one assumes the unimolecular fragmentation of $CH_3OAr^{\bullet-}M^+$ to be a single-step reaction: the delocalized negative charge in the π^* radical has to be concentrated gradually on the oxygen atom in order to evolve toward the products (either $CH_3O^-M^+ + Ar^\bullet$ in the case of ArO bond scission, or $CH_3^\bullet + M^+{}^-OAr$ in the case of CH_3O bond scission). This means that in both modes of decomposition the proximity of the metal cation lowers the energy of the transition state (cf. Figure 6), a cross-over point, to a dissociative σ^* state.[21] However, as in the ArO bond scission, the negative charge will be strictly localized on oxygen in $CH_3O^-M^+$, whereas in CH_3O bond scission it will be still rather delocalized in $M^+{}^-OAr$; the effect of lowering the activation energy by the electrical field of the cation will be more pronounced in the ArO bond scission. This effect will be the stronger, the smaller is the cationic radius. In the free anion, one would expect from the circumstances that an ArO bond is much stronger than a CH_3O bond (170 kJ mol^{-1} when Ar = C_6H_5) and only RO bond scission takes place.

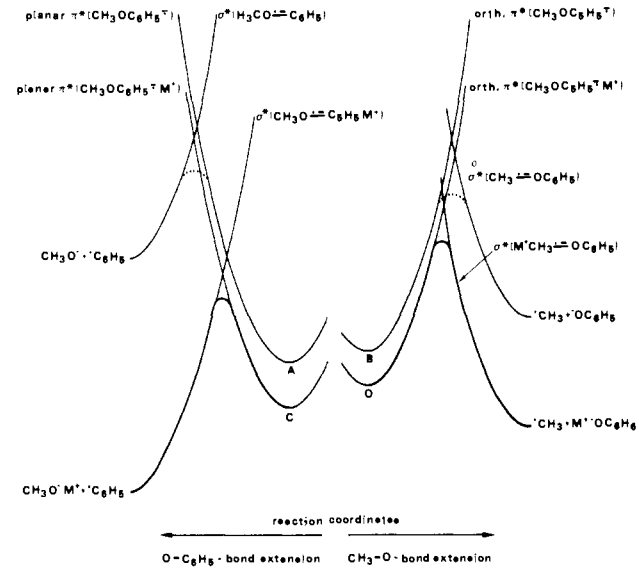

Figure 6. Schematic energy profile for the unimolecular decomposition of anisole radical anion in a hypothetical naked anion and in a contact ion pair. Points A and B as well as C and D are connected on both potential hypersurfaces by lines that correspond to rotation about a single bond. These lines that do not go through any minimum or maximum are not represented because they correspond to coordinates independent of CO bond extension.

The present study also shows that, when the radical anion is forced by steric hindrance into a conformation where the CH_3O bond is situated in a plane perpendicular to the aromatic system (cf. Figures 2(2) and 3(2)), the metal cation moves away from the oxygen atom to a position above the aromatic ring. At the same time, the electron spin density on the methyl carbon increases by a factor of more than 20 because of the $\pi-\sigma$ interaction of the aromatic system with the CH_3O bond electron pair. This weakens the CH_3O bond, and the metal cation is unable to stabilize the transition state for an ArO bond scission through its Coulomb effect. This results in preferential RO bond scission.

In terms of Figure 6, which has to be understood merely as a pictorial representation of the process, this means that the parabolic branches on the left for planar $\pi^*(CH_3OAr^{\bullet-})M^+$ will go up the large the cation is, especially in the case of $\mathbf{7}^{\bullet-}M^+$. The activation barrier for ArO bond scission increases therefore much more with the size of the cation than for RO bond scission in the orthogonal conformation, which explains the exclusive RO bond scission in $\mathbf{7}^{\bullet-}Na^+$, $\mathbf{7}^{\bullet-}K^+$ and $\mathbf{7}^{\bullet-}Cs^+$, not verified for $\mathbf{7}^{\bullet-}Li^+$.

A preparative experiment that confirms the preference for RO bond scission, when the conformation is orthogonal, is the cleavage of *tert*-butyl phenyl ether by alkali metals.[5] Apparently contradictory results of (a) preferred ArO bond scission for 1,2,3-trimethoxybenzene and 2,6-di-*tert*-butylanisole and (b) preferred RO bond scission for 2,3-dihydroisobenzofurans[5] suggest that here the products are not controlled only by the relative rates of concurrent unimolecular fragmentations but also by other factors which certainly result from the substantially different preparative reaction conditions. If these contradictions are merely apparent,

(35) Takeshita, T.; Hirota, N. *J. Am. Chem. Soc.* **1971**, *90*, 6421.

the proposed concerted unimolecular fragmentation step explains the effects of structure, conformation, counterion, and solvent on regioselectivity without any need to resort to the hypothesis of an unsubstantiated σ^* intermediate.

Experimental Section

Samples of compounds **1-3** and **5** were kindly provided by Prof. A. Maercker, **4** was purchased from Aldrich, and **6** and **7** were synthesized and purified as described in the literature.[39,40]

Tetrahydrofuran (THF) and 1,2-dimethoxyethane (DME) were distilled from a Na-K alloy in the vacuum line directly into the sample tube.

The radicals have been generated by alkali-metal reduction (Na-K alloy, Li, Na, K, and Cs) under high vacuum with standard techniques.[28]

ESR, ENDOR, and TRIPLE resonance studies were recorded on a Bruker ER 200-D instrument for ESR and a Bruker EN 810 spectrometer system for ENDOR and TRIPLE resonance.

Acknowledgment. We thank the Instituto Nacional de Investigação Cientifica (INIC), Portugal, for financial support through Centro de Processos Quimicos da Universidade Técnica de Lisboa and the Foundation Volkswagenwerke, Germany, for a copperative research grant with the University of Siegen, Professor Adalbert Maercker, University of Siegen, provided us with information on the extensive systematic preparative work of his collaborators, prior to the publication of his review article,[5] where these experiments were reported for the first time in public. We thank him for this, for sending us samples of several ethers, and for encouraging us to reopen the discussion on the mechanism of ether cleavage by alkali metals. B.J.H. also thanks Professor Andrew Streitwieser, UCLA, for a stimulating discussion.

(36) Amatore, C.; Combellas, C.; Pinson, J.; Oturan, M. A.; Robveille, S.; Savéant, J.-M.; Thiébault, A. *J. Am. Chem. Soc.* **1985**, *107*, 4846.
(37) Symons, M. C. R. *J. Chem. Soc., Chem. Commun.* **1977**, 408.
(38) Symons, M. C. R. *Pure Appl. Chem.* **1981**, *53*, 223.
(39) Willner, I.; Halpern, M. *Synthesis* **1979**, 177.
(40) Meek, J. S.; Monroe, P. A.; Bouboulis, C. J. *J. Org. Chem.* **1963**, *28*, 2572.

Deprotonation of Tertiary Amine Cation Radicals. A Direct Experimental Approach

J. P. Dinnocenzo*,† and T. E. Banach‡

Contribution from the Department of Chemistry, University of Rochester, Rochester, New York 14627. *Received March 30, 1989. Revised Manuscript Received June 26, 1989*

Abstract: The tertiary amine cation radical salt p-$An_2NCH_3^{\bullet+}AsF_6^-$ was prepared by oxidation of the corresponding amine with dioxygenyl hexafluoroarsenate. The cation radical salt was characterized by EPR spectroscopy, by magnetic susceptibility, by UV-vis spectroscopy, and by single-crystal X-ray diffraction. The reaction of the salt with quinuclidine produced at 1:1 ratio of p-An_2NCH_3 and the adduct **1**. Four possible mechanisms were considered for this reaction: a proton-transfer mechanism, an electron-transfer mechanism, and two mechanisms involving a cation radical/base complex. Stopped-flow kinetics were used to determine that the reaction rate was first-order in p-$An_2NCH_3^{\bullet+}AsF_6^-$ and first-order in quinuclidine. A comparison of the reaction rate for p-$An_2NCH_3^{\bullet+}AsF_6^-$ vs p-$An_2NCD_3^{\bullet+}AsF_6^-$ provided an isotope effect of 7.68 (7) at 15.1 °C. The combined kinetic data ruled out all but a rate-limiting proton-transfer mechanism. The temperature dependence of the reaction rate provided activation parameters for the deprotonation: $\Delta H^{\ddagger}$ = 3.7 (1) kcal/mol and $\Delta S^{\ddagger}$ = -22.3 (4) cal/mol·deg. Reaction of p-$An_2NCH_3^{\bullet+}AsF_6^-$ with four substituted quinuclidine bases provided a Brønsted β of 0.63. The isotope effects for reaction with the substituted quinuclidine bases were measured, and a plot of k_H/k_D vs pK_a was found to have a maximum ca. 8 pK_a units lower than the pK_a of the cation radical. This was explained in terms of the differing widths of the potential energy wells for the X-H bonds being broken and being made.

Deprotonation at carbon is a commonly proposed reaction for many organic cation radical intermediates. For example, this is the generally accepted fate of alkylaromatic and tertiary amine cation radicals generated in chemical,[1] electrochemical,[2] photochemical,[3] and even some enzymatic oxidation reactions.[4] Despite their importance, these proton-transfer reactions are still poorly understood vis-à-vis comparable proton transfers from even electron molecules.

Part of the difficulty in probing cation radical deprotonations is that they are often masked by prior electron-transfer steps. In order to extract kinetic data regarding the deprotonation step, it is usually necessary to make some sort of approximation. For example, consider the frequently encountered kinetic scheme shown below. For situations where the deprotonation step is rate-limiting, one needs to know either the electron-transfer equilibrium constant (k_1/k_{-1}) or the rate constant for the back-electron-transfer step (k_{-1}) in order to relate the observed reaction rate constant to the deprotonation rate constant (k_2). In practice, this is often difficult to do. One of the problems is that thermodynamically meaningful oxidation potentials are difficult to obtain for the substrates of interest.[5]

$$RH + oxd \underset{k_{-1}}{\overset{k_1}{\rightleftharpoons}} RH^{\bullet+} + red \xrightarrow[B]{k_2} R^{\bullet} + HB^+$$

We have been exploring a way to more directly examine the deprotonation of organic cation radicals that circumvents the

† Fellow of the Alfred P. Sloan Foundation, 1988-90.
‡ Weissberger Fellow, 1987-88.

(1) Alkylaromatics: (a) Schlesener, C. J.; Amatore, C.; Kochi, J. K. *J. Am. Chem. Soc.* **1984**, *106*, 7472 and references therein. Tertiary amines: (b) Chow, Y. L.; Danen, W. C.; Nelsen, S. F.; Rosenblatt, D. H. *Chem. Rev.* **1978**, *78*, 243 and references therein.
(2) Alkylaromatics: (a) Nyberg, K. In *Encyclopedia of Electrochemistry of the Elements*; Bard, A. J., Lund, H., Eds.; Marcel Dekker: New York, 1978; Vol. XI, Chapter IX-1, p 43. (b) Eberson, L.; Nyberg, K. *Acc. Chem. Res.* **1973**, *6*, 106. (c) Baumberger, R. S.; Parker, V. D. *Acta Chem. Scand., Ser. B* **1980**, *B34*, 537. (d) Bewick, A.; Edwards, G. J.; Mellor, J. M.; Pons, S. *J. Chem. Soc., Perkin Trans. 2* **1977**, 1952. Tertiary amines: (e) Weinberg, N. L.; Weinberg, H. R. *Chem. Rev.* **1968**, *68*, 449. (f) Mann, C. K.; Barnes, K. K. *Electrochemical Reactions in Nonaqueous Systems*; Marcel Dekker: New York, 1970; Chapter 9. (g) Masui, M.; Sayo, H. *J. Chem. Soc. B* **1971**, 1593.
(3) Alkylaromatics: (a) Mariano, P. S.; Stavinola, J. L. In *Synthetic Organic Photochemistry*; Horspool, W. M., Ed.; Plenum Press: New York, 1984; Chapter 3 and references therein. (b) Lewis, F. D. *Acc. Chem. Res.* **1986**, *19*, 401 and references therein. Tertiary amines: (c) Cohen, S. G.; Parola, A.; Parsons, G. H., Jr. *Chem. Rev.* **1973**, *73*, 141. (d) Wagner, P. J. *Top. Curr. Chem.* **1976**, *66*, 1. (e) Davidson, R. S. *Adv. Phys. Org. Chem.* **1983**, *19*, 1. (f) Reference 3a. (g) Reference 3b. (h) Kavarnos, G. J.; Turro, N. J. *Chem. Rev.* **1986**, *86*, 401.

0002-7863/89/1511-8646$01.50/0